

Periodically Driven Array of Single Rydberg Atoms

Sagarika Basak, Yashwant Chougale and Rejish Nath
 Indian Institute of Science Education and Research, Pune 411 008, India

An array of single Rydberg atoms driven by a frequency modulated light field is studied. The periodic modulation effectively modifies the Rabi coupling, leading to unprecedented dynamics in the presence of Rydberg-Rydberg interactions. They include state dependent population trapping, the Rydberg blockade for small and anti-blockades at large interaction strengths. Interestingly, the Schrieffer-wolf transformation reveals a fundamental process in Rydberg gases, correlated Rabi oscillations, arising from the long-range interactions, provides an alternative depiction for Rydberg blockade and it exhibits a nontrivial behaviour in the presence of periodic modulation. The dynamical localization of a many body configuration in a driven Rydberg-lattice is discussed.

Controlled coherent quantum dynamics is a great challenge and provides the impetus for various studies in diverse systems; in particular, periodically driven or Floquet systems [1, 2]. They exhibit a wealth of quantum phenomena, in single particle case, the noted ones are the coherent destruction of tunneling [3], dynamic localization in quantum transport [4], population trapping (PT) in a two-level system (TLS) [5, 6] and Landau-Zener-Stückelberg (LZS) interference [2, 7, 8]. The latter happens when the TLS is driven periodically across an avoided crossing such that separate Landau-Zener transitions (LZTs) interfere [2, 10], also demonstrated using Rydberg atoms [6, 19]. The quantum interference plays a decisive role in above studies. Extending to many-body systems, complex scenarios emerge, for instance, dynamical-freezing [11], -synchronization [12], and -localization [13], as shown in driven quantum spin systems. Also, ergodicity breaking or many body localization in driven quantum systems has been the subject of intense theoretical studies [14], and recently, probed experimentally in a lattice of interacting ultracold fermions [15]. On a bigger perspective, they constitute a platform to explore non-equilibrium quantum states [16] and topological phenomena [17], including the time crystals [18].

On the other side, ultra-cold Rydberg gases [19] offer a manifold of prospects to probe quantum physics [20], owing to their exaggerated properties [19], supported by the experimental developments [21]; in particular, recent realizations of Rydberg-atomic arrays [22, 23]. A Rydberg setup typically involves laser fields coupling the ground state $|g\rangle$ with one or more Rydberg states $|e\rangle$. At very low temperatures, the strong interactions among the Rydberg atoms lead us to describe the internal-states dynamics in the frozen gas limit, where the motional degrees of freedom are neglected [24]. The level shifts caused by the interactions suppress further excitations within a finite volume is called the Rydberg blockade [25, 26]. The latter brings up the *super-atom* picture, in which a fully blocked ensemble of N atoms exhibits Rabi oscillations between the ground state $|G\rangle = \otimes_{i=1}^N |g^{(i)}\rangle$ and the collective single excitation $|+\rangle = \sum_i |gg\dots e^{(i)}\dots gg\rangle / \sqrt{N}$ [27]. It has been proposed to generate entangled mesoscopic ensembles for fast quantum gate operations [25].

In this letter, we examine a chain of single atoms driven by a frequency modulated field, which couples $|g\rangle$ to $|e\rangle$. The periodic modulation effectively modifies the Rabi couplings and

together with Rydberg-Rydberg interactions unprecedented scenarios emerge. For instance, the Rydberg blockade exists even for interactions weaker compared to single atom Rabi coupling, resonant excitation of $|ee\rangle$ at large interactions (anti-blockade), and state dependent PT. The blockade enhancement offers the possibility of entangling two atoms at large separations without altering the bare Rabi frequency. The anti-blockade in a non-driven setup demands a three-level scheme [28] or a zero-area phase jump pulse [29], but the population in $|ee\rangle$ is found to be very small [28], which can be significantly augmented in a driven system. Interestingly, employing the Schrieffer-wolf transformation [31] reveals a qualitatively novel feature, *correlated* Rabi-oscillations, arising from the long-range nature of the interactions, analogous to density assisted hopping in optical lattices [30]. Correlated Rabi coupling (CRC) provides an alternative depiction for Rydberg blockade. Finally, we discuss the interaction dependent dynamical localization of a many-body configuration, which may pave a way towards exploring ergodic-nonergodic transitions using periodically driven Rydberg chains.

Model. We consider an one dimensional array with one atom per site, in which the electronic ground state $|g\rangle$ is coupled to a Rydberg state $|e\rangle$ via a light field with its frequency modulated periodically in time t . The system is described in the frozen gas limit, by the Hamiltonian:

$$\hat{H} = -\hbar\Delta(t) \sum_{i=1}^N \hat{\sigma}_{ee}^i + \frac{\hbar\Omega}{2} \sum_{i=1}^N \hat{\sigma}_x^i + \sum_{i<j} V_{ij} \hat{\sigma}_{ee}^i \hat{\sigma}_{ee}^j, \quad (1)$$

where $\hat{\sigma}_{ab} = |a\rangle\langle b|$ with $a, b \in \{e, g\}$, $\hat{\sigma}_x = \hat{\sigma}_{eg} + \hat{\sigma}_{ge}$, Ω is the Rabi frequency, $\Delta(t) = \Delta_0 + \delta \sin \omega_0 t$ is the time-dependent detuning with amplitude $\delta > 0$ and the modulation frequency ω_0 . An alternative way to introduce periodic $\Delta(t)$ is to drive the Rydberg state using a modulated microwave field [8], which off-resonantly couples to a nearby Rydberg state [6]. The Rydberg excited atoms interact via the strong van der Waals interactions, $V(r) = C_6/r^6$ [32]. We solve numerically the Schrödinger equation: $i\hbar\partial/\partial t|\psi\rangle = \hat{H}(t)|\psi\rangle$ and analyze the dynamics. Henceforth we take $\hbar = 1$.

To gain an insight, especially at large ω_0 or interactions, we move to a rotating frame [31]: $|\psi'\rangle = \hat{U}(t)|\psi\rangle$ where $\hat{U}(t) = \exp[i f(t) \sum_j \hat{\sigma}_{ee}^j + i t \sum_{j<k} V_{jk} \hat{\sigma}_{ee}^j \hat{\sigma}_{ee}^k]$ with $f(t) = \delta/\omega_0 \cos \omega_0 t - \Delta_0 t$. The new Hamiltonian, $\hat{H}'(t) =$

$\hat{U}\hat{H}\hat{U}^\dagger - i\hbar\hat{U}\hat{U}^\dagger$, after using the Jacobi-Anger expansion $\exp(\pm iz \cos \omega_0 t) = \sum_{m=-\infty}^{\infty} J_m(z) \exp(\pm im[\omega_0 t + \pi/2])$, is [33]

$$\hat{H}' = \frac{\hbar\Omega}{2} \sum_{j=1}^N \sum_{m=-\infty}^{\infty} i^m J_m(\alpha) \left(g(t) e^{i \sum_{k \neq j} V_{jk} \hat{\sigma}_{ek}^k} \hat{\sigma}_{eg}^j + \text{H.c.} \right) \quad (2)$$

where $J_m(\alpha)$ is the m th order Bessel function with $\alpha = \delta/\omega_0$ and $g(t) = \exp[i(m\omega_0 - \Delta_0)t]$. As seen in Eq. (2), the periodic detuning has effectively modified the Rabi coupling.

Single atom. Hinge on Ω , δ and ω_0 , we consider three regimes [5, 34]. (i) The weak driving limit: $\delta \ll \Omega_{eff} \equiv \sqrt{\Omega^2 + \Delta_0^2}$, the resonant $|g\rangle$ to $|e\rangle$ transition occurs at $\omega_0 = \Omega_{eff}$ with an effective Rabi frequency $\Omega' = \delta \sin(\tan^{-1}[\Omega/\Delta_0])$ [34]. (ii) The high-frequency limit (HFL): $\omega_0 \gg \Omega$, the only term relevant in $\sum_{m=-\infty}^{\infty} (\cdot)$ in Eq. (2) at longer times gives the resonance $m\omega_0 = \Delta_0$, with $\Omega' \approx \Omega |J_m(\alpha)|$. If $\Delta_0 = 0$, $\Omega' = \Omega J_0(\alpha)$, hence at $J_0(\alpha) = 0$, the PT happens [5, 6]. (iii) The fast passage limit (FPL): $\omega_0 \sqrt{\delta^2 - \Delta_0^2} \gg \Omega^2$ with $\delta - \Delta_0 \gg \Omega$, the resonance is at

$$n\omega_0 = \Delta_0 \text{ with } \Omega' = (2\omega_0/\pi) |\cos(\theta - \pi/4)| \sqrt{\frac{\pi\Omega^2}{2\omega_0} / \sqrt{\delta^2 - \Delta_0^2}},$$

where $\omega_0\theta = \sqrt{\delta^2 - \Delta_0^2} - \Delta_0 \cos^{-1} \frac{\Delta_0}{\delta}$ [34]. The PT occurs if $\cos(\cdot) = 0$. Both HFL and FPL co-exist for $\delta, \omega_0 \gg \Omega$. In the FPL, the system is driven past an avoided level crossing repeatedly, causing non-adiabatic LZTs. The transfer matrix (TM) method based on adiabatic-impulse model [2, 34] gives a good description. Around the avoided crossing, the LZTs are given by a non-adiabatic unitary operator \hat{G}_{LZ} and away from it, an adiabatic phase evolution through \hat{G}_j with j being left ($j = 1$) or right ($j = 2$) of the crossing. Then, the total phase acquired during a full cycle provides the resonant conditions.

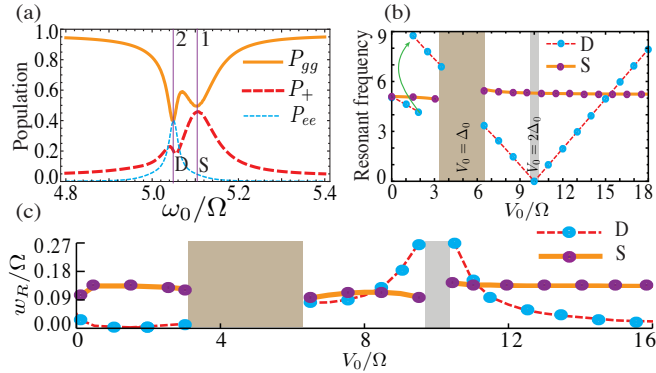


Figure 1. (color online). The results for $N = 2$ in the weak driving limit with $\delta = 0.4\Omega$ and $\Delta_0 = 5\Omega$. (a) $P_\beta(t)$ vs ω_0 with $|\beta\rangle \in \{|gg\rangle, |+\rangle, |ee\rangle\}$ for $V_0 = 0.1\Omega$ and $\Omega T_f = 1000$. The vertical lines 1 and 2 indicate resonances S and D respectively. (b) ω_S/Ω (solid lines) and ω_D/Ω (dashed lines) vs V_0 and the numerical results are shown by filled circles. (c) the widths, w_R of resonances vs V_0 .

$N = 2$. The interactions, $V(r_{12}) = C_6/a^6 \equiv V_0$, where a is the lattice spacing, significantly modifies the resonance criteria as well as the excitation dynamics. In particular, we focus

at the resonance criteria for $|gg\rangle \leftrightarrow |+\rangle = (|eg\rangle + |ge\rangle)/\sqrt{2}$ (S) and $|gg\rangle \leftrightarrow |ee\rangle$ (D) transitions. S and D indicate single and double excitations respectively. Numerically, they are obtained as the peaks/dips in the time averaged populations: $P_\beta = (1/T_f) \int_0^{T_f} |\langle \beta | \psi(t) \rangle|^2 dt$; $|\beta\rangle \in \{|gg\rangle, |ee\rangle, |+\rangle\}$, as a function of ω_0 , with an initial state $|I\rangle = |gg\rangle$ [see Fig.1(a) and (b)].

Weak driving limit. For $V_0 \ll \Omega_{eff}$, [Fig.1(a)], the atoms are assumed non-interacting, and V_0 is account through an effective detuning, $\Delta'_0 = \Delta_0 - V_0/2$ for $|ee\rangle$. Thus, the resonances occur at $\omega_0 = \omega_S = \Omega_{eff}$ and $\omega_0 = \omega_D = \sqrt{\Omega^2 + (\Delta'_0)^2}$ for S and D transitions respectively. If S and D are sufficiently apart in ω_0 , at S , the periodic driving results in Rydberg-blockade despite small V_0 [$V_0 = 0.1\Omega$ in Fig.1(a)]. This *blockade enhancement* (BE) becomes more apparent later when we analyze HFL or FPL with $\Delta_0 = 0$. Note that, the blockade exists only if $V_0 > \Omega$ for $\delta = \Delta_0 = 0$.

Increasing V_0 , and when $V_0 \sim \Omega_{eff}$, the non-interacting picture fails, results a jump in ω_D to a higher value [Fig.1(b)]. Note that, here, ω_S and ω_D are provided by the difference in the eigenvalues of the non-driven \hat{H} ($\delta = 0$). The eigenstates can be approximated to $|gg\rangle$, $|+\rangle$ and $|ee\rangle$ if $\Delta_0 \gg \Omega$, except when $V_0 \approx \Delta_0$ and $V_0 \approx 2\Delta_0$ [shaded regions in Fig. 1(b)-(c)]. Obtaining the eigenvalues up to fourth order in Ω , we have

$$\omega_S = |E_{gg} - E_{+}| \approx \Delta_0 + \frac{\Omega^2}{2} \left(\frac{2}{\Delta_0} - \frac{1}{\Delta_0 - V_0} \right) + \mathcal{O}(\Omega^4) \quad (3)$$

$$\omega_D = |E_{gg} - E_{ee}| \approx |V_0 - 2\Delta_0 - \frac{\Omega^2}{2} \left(\frac{2}{\Delta_0} + \frac{1}{\Delta_0 - V_0} \right) + \frac{\Omega^4}{4} \left(\frac{1}{\Delta_0^3} + \frac{1}{(\Delta_0 - V_0)^3} \right)|. \quad (4)$$

Eqs. (3) and (4) [dashed and solid lines in Fig. 1(c)] are in excellent agreement with the numerical results. The jump in ω_D near $V_0 \sim \Omega_{eff}$ is not an abrupt one, but with a small co-existence region. When $V_0 \approx \Delta_0$ both $|+\rangle$ and $|ee\rangle$ are almost degenerate, and the resonances S and D as such do not exist, since the population is shared among both $|+\rangle$ and $|ee\rangle$ from $|gg\rangle$. For large values of V_0 , ω_S becomes independent of V_0 , whereas ω_D decreases and vanishes at $V_0 \approx 2\Delta_0$ and then increases linearly with V_0 . When $V_0 \approx 2\Delta_0$, $|gg\rangle$ and $|ee\rangle$ are almost degenerate, hence D resonance exists even for $\delta = 0$, but not S . The two resonances cross near $V_0 \sim 3\Delta_0 + 3\Omega^2/\Delta_0$. The resonance widths w_R are obtained by a Lorentzian fit [Fig.1(c)]. As V_0 increases, D gets progressively narrower making the higher order terms in Eq. (4) relevant, and its existence at large $V_0 (> 2\Delta_0)$ is interpreted as the anti-blockade.

HFL. The dynamics is better understood by writing the Hamiltonian in Eq. (2) for $N = 2$ as [33]

$$\hat{H}^{(2)} = \frac{\Omega}{2} \sum_{m=-\infty}^{\infty} i^m J_m(\alpha) g(t) \left(\sum_{j=1}^2 \hat{\sigma}_{eg}^j + (\hat{\sigma}_{eg}^1 \hat{\sigma}_{ee}^2 + \hat{\sigma}_{eg}^2 \hat{\sigma}_{ee}^1) (e^{iV_0 t} - 1) \right) + \text{H.c.} \quad (5)$$

A close inspection on Eq. (5) reveals that \hat{H}' consists of

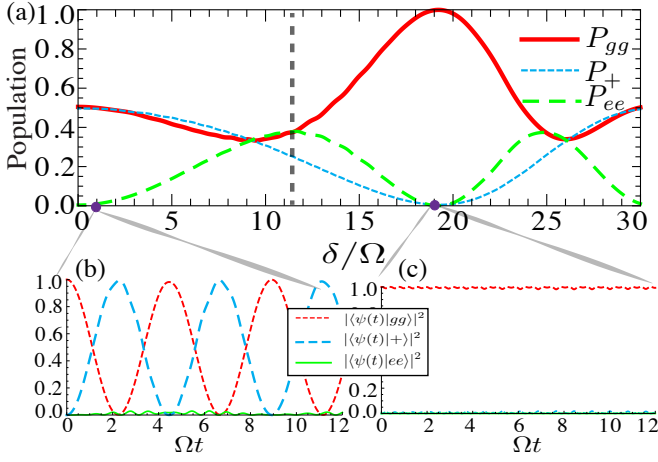


Figure 2. (color online). (a) P_α vs δ for $N = 2$ in the HFL with $n_1 = 0$, $n_2 = -1$ ($\omega_0 = V_0 = 8\Omega$) and $\Omega T_f = 100$. At the vertical dashed line ($\delta = 11.476\Omega$) $J_0(\alpha) \sim J_{-1}(\alpha)$. (b) and (c) show the dynamics for $\delta = \Omega$ and $\delta = 19.24\Omega$ respectively.

only off-diagonal elements correspond to $|gg\rangle \leftrightarrow |+\rangle$ and $|+\rangle \leftrightarrow |ee\rangle$ transitions, with respective resonance criteria: (i) $n_1\omega_0 = \Delta_0$ and (ii) $n_2\omega_0 = \Delta_0 - V_0$. Taking large V_0 such that the two resonances do not overlap in ω_0 , the *quantum interference* plays an important role. If condition (i) is met, the transition amplitudes for $|gg\rangle \leftrightarrow |+\rangle$ interfere constructively (S resonance), whereas that of $|+\rangle \leftrightarrow |ee\rangle$ interfere destructively. The opposite is true if (ii) is satisfied. Thus, the dynamics depends crucially on the initial state. For instance, if $|I\rangle = |ee\rangle$, the condition (ii) leads to the coherent ROs between $|ee\rangle$ and $|+\rangle$ with $\Omega' = 2\Omega J_{n_2}(\alpha)$, where as PT takes place if $|I\rangle = |gg\rangle$. The state dependent PT emerges as a unique feature from the Rydberg interactions. To satisfy (i) and (ii) simultaneously, we require $n_1 \neq n_2$, which leaves δ as the only free parameter. In Fig. 2(a) we show the dynamics vs δ for $n_1 = 0$, $n_2 = -1$, with $V_0 = 8\Omega$, $\omega_0 = 8\Omega$ and $|I\rangle = |gg\rangle$. At $\delta = 0$ there exists Rydberg blockade, and also the blockade occurs whenever $J_{n_1}(\alpha) \gg J_{n_2}(\alpha)$ for $\delta \neq 0$ with $\Omega' = 2\Omega \sqrt{J_0^2(\alpha) + J_{-1}^2(\alpha)}$ [Fig. 2(b)]. If $J_0(\alpha) \sim J_{-1}(\alpha)$ the anti-blockade occurs, shown by dashed vertical line in Fig. 2(a). And, PT is shown at $J_0(\alpha) \sim 0$ [Fig. 2(c)].

If $\delta \gtrsim \Omega$ the HFL merges with FPL [34] for $\Delta_0 = 0$. The existence of multi-LZTs makes the TM method cumbersome, but for $V_0 \gg \Omega_{eff}$, they are well separated in Δ_0 axis. This allows us to separate the adiabatic and non-adiabatic regions and obtain the respective resonance criteria [33]. Doing so, we get $\Delta_0 = n\omega_0$ for S resonance with $\Omega' = (2\omega_0/\pi)|\cos(\theta - \pi/4)|\sqrt{\frac{\pi\Omega^2}{\omega_0}/\sqrt{\delta^2 - \Delta_0^2}}$. The resonance condition for $|+\rangle \leftrightarrow |ee\rangle$ is $\Delta_0 - V_0 = n\omega_0$ with $\Omega' = (2\omega_0/\pi)|\cos(\tilde{\theta} - \pi/4)|\sqrt{\frac{\pi\Omega^2}{\omega_0}/\sqrt{\delta^2 - (\Delta_0 - V_0)^2}}$ where $\omega_0\tilde{\theta} = \sqrt{\delta^2 - (\Delta_0 - V_0)^2} - (\Delta_0 - V_0)\cos^{-1}\frac{\Delta_0 - V_0}{\delta}$ and that of D resonance is $\Delta_0 - V_0/2 = n\omega_0$. They are in agreement with the numerical solutions of Eq. (1). Fig. 3 shows P_{ee}

vs V_0 in the FPL with $|I\rangle = |gg\rangle$ and $\Delta_0 = 0$. When $\delta = 0$, P_{ee} decreases monotonously (thin line) exhibiting the Rydberg blockade ($P_{ee} \sim 0$) at large V_0 , whereas in the presence of driving (thick line) it exhibits a non-monotonous character. The initial faster decay of P_{ee} indicates the BE and the periodic peaks at higher V_0 show anti-blockades. The peaks can be shifted in V_0 as well as made higher or narrower by taking $\Delta_0 \neq 0$ (dashed line). The BE at small V_0 and anti-blockades at large V_0 may have far reaching consequences in the dynamics of periodically driven Rydberg ensembles. Also, we have verified that the two features persists in the presence of spontaneous emission [33].

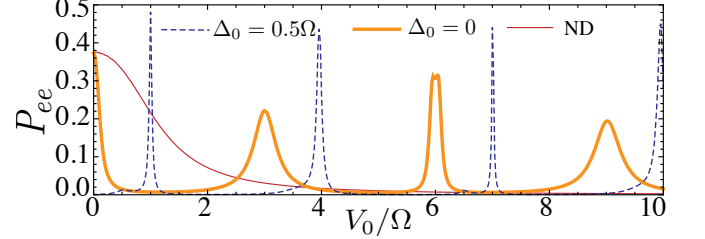


Figure 3. (color online). P_{ee} vs V_0 in FPL, with $\Omega T_f = 300$, $\omega_0 = 3\Omega$ and $\delta = 34\Omega$. Thin and thick solid lines are for non-driven and driven cases respectively with $\Delta_0 = 0$. The dashed line is for $\Delta_0 = 0.5\Omega$.

CRC. Interestingly, the last two terms in Eq. (5) reveal CRC as a fundamental process in Rydberg gases, emerging from the long-range interactions, essentially driving $|+\rangle \leftrightarrow |ee\rangle$ transition. It is also apparent in the period-averaged or the zeroth order Floquet Hamiltonian [33, 35] $H_{eff} = 1/T \int_0^T dt \hat{H}^{(2)}(t)$, where $T = 2\pi/\omega_0$ if $\omega_0 \gg V_0$ or $T = 2\pi/V_0$ if $V_0 \gg \omega_0$. Henceforth, we take $\Delta_0 = 0$ (S -resonance). For $\omega_0 \gg V_0$:

$$\hat{H}_{eff}^{\omega_0 \gg V_0} = \frac{\Omega}{2iT} \sum_{m=-\infty}^{\infty} i^m J_m(\alpha) \frac{(e^{iV_0 T} - 1)}{m\omega_0 + V_0} \hat{X} + \frac{J_0(\alpha)\Omega}{2} \left(\sum_{j=1}^2 \hat{\sigma}_{eg}^j - \hat{X} \right) + \text{H.c.}, \quad (6)$$

where $\hat{X} = \hat{\sigma}_{ee}^1 \hat{\sigma}_{eg}^2 + \hat{\sigma}_{ee}^2 \hat{\sigma}_{eg}^1$. For $V_0 \ll \Omega, \omega_0$, we take $m\omega_0 + V_0 \approx m\omega_0$ in Eq. (6), which lead us to $\hat{H}_{eff}^{\omega_0 \gg V_0} \approx J_0(\alpha)\Omega/2 \sum_j \hat{\sigma}_{eg}^j + i[\Omega J_0(\alpha)V_0 T/4]\hat{X} + \mathcal{O}(V_0^2) + \text{H.c.}$. Hence, for small interactions the CRC increases linearly with V_0 . Similarly, for $V_0 \gg \omega_0$:

$$\hat{H}_{eff}^{V_0 \gg \omega_0} = \frac{\Omega}{2iT} \sum_{m=-\infty}^{\infty} i^m J_m(\alpha) (e^{im\omega_0 T} - 1) \left[\sum_{j=1}^2 \frac{\hat{\sigma}_{eg}^j}{m\omega_0} + \left(\frac{1}{m\omega_0 + V_0} - \frac{1}{m\omega_0} \right) \hat{X} \right] + \text{H.c.} \quad (7)$$

Eqs. (6) and (7) govern the time evolution of the system at integer multiple of the period T . For small amplitude modulations ($\delta \ll 1$), only $m = 0, \pm 1$ have significant contributions in Eq. (7), and we get $\hat{H}_{eff}^{V_0 \gg \omega_0} \approx \chi(\sum_j \hat{\sigma}_{eg}^j - \hat{X}) + \text{H.c.}$ with $\chi = \Omega[J_0(\alpha) + 2iJ_1(\alpha)]/2$, interestingly, which provides

an alternative perspective for Rydberg blockade. The -ve sign in front of \hat{X} implies that it is the *correlated Rabi coupling* which results in blockade at large V_0 , by completely suppressing the single atom Rabi coupling thereby we have $\langle + | \hat{H}_{eff}^{V_0 > \omega_0} | ee \rangle = 0$. Further, we look at the two-body correlation, $\bar{C}_{x2} = 1/T_f \int_0^{T_f} C_{x2}(t) dt$ with $C_{x2}(t) = \langle \psi(t) | (\hat{\sigma}_x^1 \hat{\sigma}_{ee}^2 + \hat{\sigma}_x^2 \hat{\sigma}_{ee}^1) | \psi(t) \rangle / 2$ with $|I\rangle = |gg\rangle$ as a function of V_0 , see Fig. 4(a). Its magnitude measures the probability of finding second atom in the Rydberg state while first atom making a transition. When $\delta = 0$, for small V_0 the \bar{C}_{x2} increases with V_0 until it reaches a maximum and then decays as $1/V_0$ due to the Rydberg blockade. The periodic modulation ($\delta \neq 0$) results in a non-trivial behaviour for \bar{C}_{x2} , particularly the non-periodic oscillations between +ve and -ve values. Since $\Delta_0 = 0$, at $V_0 = n\omega_0$ both $|+\rangle \leftrightarrow |ee\rangle$ and $|+\rangle \leftrightarrow |gg\rangle$ transitions are at resonance which is identical to the case of $V_0 = 0$, hence effectively $\bar{C}_{x2} = 0$. Also \bar{C}_{x2} vanishes when $P_{ee} = 0$ making its oscillatory nature.

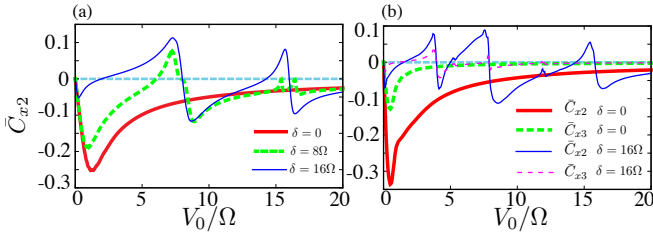


Figure 4. (color online). Correlations vs V_0 for (a) $N = 2$ and (b) $N = 10$. For both figures $\Delta_0 = 0$, $\omega_0 = 8\Omega$ and $\Omega T_f = 150$.

$N > 2$. More resonances appear with increasing N [36]. The S resonance ($|G\rangle \leftrightarrow |+\rangle$) is independent of N and V_0 , but a large V_0 is required to isolate it from other resonances. Higher-order correlations, $C_{x2}(t) = \langle \sum_j (\hat{\sigma}_x^j \hat{\sigma}_{ee}^{j+1} + \hat{\sigma}_x^j \hat{\sigma}_{ee}^{j-1}) \rangle / N$ and $C_{x3}(t) = \langle \sum_j (\hat{\sigma}_x^j \hat{\sigma}_{ee}^{j+1} \hat{\sigma}_{ee}^{j-1}) \rangle / N$ for $N = 10$ are shown in Fig. 4(b). As expected \bar{C}_{x3} is smaller and decays faster with V_0 compared to \bar{C}_{x2} . As N increases, the correlations exhibit additional oscillations due to the participation of more resonances.

In a similar vein, where the dynamical localization of a condensate in a periodically shaken lattice by suppressing the tunnelling is observed [37], we analyze that of a many-body configuration. We take $|I\rangle = |\dots g, e, g, \dots\rangle$, a singly excited state as depicted in Fig. 5(a). The localization of $|I\rangle$ in a given eigen-basis can be measured in terms of either survival probability, $|\langle I | \psi(t) \rangle|^2$ [38] or the inverse participation ratio, $I_\psi(t) = \sum_i p_i^2(t)$ [39], where $p_i(t)$ is the probability of finding the system in the i^{th} eigen state. We choose the eigen states of $\hat{H}(\Omega = 0, \delta = 0)$ as the basis for our calculations. In the absence of periodic modulation, for small N [dashed line in Fig. 5(b)] one observes collapse and partial revivals of $|I\rangle$ [23]. As N increases, the collapse becomes faster and eventually no revival due to the exponential growth in the dimensions of the Hilbert space. In contrast, the periodic modulation may significantly slow down the collapse, leading to the dynamical

localization or stabilization of $|I\rangle$.

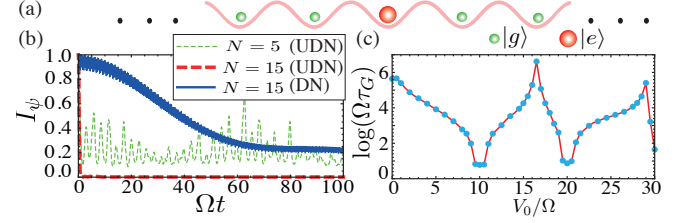


Figure 5. (color online). The results for dynamical stabilization. (a) The initial configuration with one excitation at the centre of the lattice. (b) I_ψ vs time for both driven (DR) and undriven (UDR) cases with $V_0 = 5\Omega$. For driven case, $\delta = 24.0483\Omega$ and $\omega_0 = 10\Omega$ which give $J_0(\delta/\omega_0) = 0$. (c) The log of the temporal width τ_G vs V_0 for $N = 15$.

For $\delta \neq 0$, I_ψ exhibits a Gaussian decay [40] in t [the solid line in Fig. 5(b)], and the oscillation in the profile is attributed to the LZS interference. Strikingly, similar Gaussian decay of initial state is shown in the quench dynamics of isolated quantum Hamiltonians, when $|I\rangle$ has a Gaussian distribution over the eigen states of the final Hamiltonian [38]. The Gaussian width τ_G is found to be independent of N for sufficiently large value of $N (> 5)$, but depends crucially on V_0 [Fig. 5(c) shows $\log_{10} \tau_G$ vs V_0 for $N = 15$] as well as the driving parameters. Since $\Delta_0 = 0$, choosing $J_0(\delta/\omega_0) = 0$ suppress any population transfer to $|G\rangle$ from $|I\rangle$. The transitions to states with $N_e > 1$ strongly depends on V_0 . At $V_0 = n\omega$, there is a resonant transition from $|I\rangle$ to doubly excited states with excitations at the nearest sites causing the minima in τ_G . Between those minima, τ_G acquires a maximum due to the Blockade effect at large interactions.

Experimental Parameters. Taking $\Omega = 2\pi \times 1$ MHz, our studies involve $\delta \sim 2\pi \times 0 - 40$ MHz, $\omega_0 \sim 2\pi \times 0 - 15$ MHz, over a maximum time, $T_f \sim 100 - 300 \mu s$ in the HFL or FPL. Note that for $n \sim 80$, the Rubidium nS state has a life time of $600 \mu s$ (or the decay constant $\Gamma = 2\pi \times 0.00167\Omega$) [41]. In the supplemental material, we show the results for BE and anti-blockade at large V_0 for $N = 2$ and $\Gamma = 0.01\Omega$, [33] which corresponds to $45S$ state of Rubidium if $\Omega = 1$ MHz.

Conclusions and outlook. Driving the detuning periodically relaxes the requirements to observe Rydberg Blockade and anti-blockade, thereby acquiring a huge controllability over the quantum dynamics in Rydberg atomic lattices. Our analysis reveals CRC as a novel feature in Rydberg chains, which can be extended as a general characteristic of two level systems with long-range interactions. Further, CRC provides an alternative and a different depiction of Rydberg blockade.

Our work offers an extra dimension to the problems that can be addressed using Rydberg atomic chains. In particular, the localization of a many-body state addressed in our studies can be extended to analyze ergodic-nonergodic transitions, in the presence of disorder. In other words, how heating takes place in such systems under periodic forcing, especially the role of long-range interactions can be probed. The stability (growth and melting) of Rydberg crystals [42] under periodic

modulation would also be a question of immediate interest due to the state of the art experiments.

Acknowledgments:- We acknowledge fruitful discussions with Weibin Li, Vijay Shenoy, Igor Lesanovsky and especially, Anatoli Polkovnikov. R.N. acknowledges the funding by the Indo-French Centre for the Promotion of Advanced Research (CEFIPRA) and support from the UKIERI-UGC Thematic Partnership No. IND/CONT/G/16-17/73UKIERI-UGC project. S.B. acknowledges the support from the Department of Science and Technology (DST), Government of India through the INSPIRE SHE Programme (8S/2012).

-
- [1] S. Kohler, J. Lehmann, and P. Hänggi, *Phys. Rep.* **406**, 379 (2005); M. P. Silveri, J. A. Tuorila, E. V. Thuneberg, and G. S. Paraoanu, *Rep. Prog. Phys.* **80**, 056002 (2017); M. Grifoni and P. Hänggi, *Phys. Rep.* **304**, 229 (1998).
- [2] S. Shevchenko, S. Ashhab, and F. Nori, *Phys. Rep.* **492**, 1 (2010).
- [3] F. Grossmann, T. Dittrich, P. Jung, and P. Hänggi, *Phys. Rev. Lett.* **67**, 516 (1991).
- [4] S. Raghavan, V. M. Kenkre, D. H. Dunlap, A. R. Bishop, and M. I. Salkola, *Phys. Rev. A* **54**, R1781 (1996).
- [5] G. S. Agarwal and W. Harshawardhan, *Phys. Rev. A* **50**, R4465 (1994); B. M. Garraway and N. V. Vitanov, *Phys. Rev. A* **55**, 4418 (1997).
- [6] M. W. Noel, W. M. Griffith, and T. F. Gallagher, *Phys. Rev. A* **58**, 2265 (1998).
- [7] J. R. Rubbmark, M. M. Kash, M. G. Littman, and D. Kleppner, *Phys. Rev. A* **23**, 3107 (1981); W. D. Oliver, Y. Yu, J. C. Lee, K. K. Berggren, L. S. Levitov, and T. P. Orlando, *Science* **310**, 1653 (2005); M. Sillanpää, T. Lehtinen, A. Paila, Y. Makhlin, and P. Hakonen, *Phys. Rev. Lett.* **96**, 187002 (2006); C. S. E. van Ditzhuijzen, A. Tauschinsky, and H. B. van Linden van den Heuvell, *Phys. Rev. A* **80**, 063407 (2009); F. Forster, G. Petersen, S. Manus, P. Hänggi, D. Schuh, W. Wegscheider, S. Kohler, and S. Ludwig, *Phys. Rev. Lett.* **112**, 116803 (2014); J. Zhou, P. Huang, Q. Zhang, Z. Wang, T. Tan, X. Xu, F. Shi, X. Rong, S. Ashhab, and J. Du, *Phys. Rev. Lett.* **112**, 010503 (2014); M. P. Silveri, K. S. Kumar, J. Tuorila, J. Li, A. Vepsäläinen, E. V. Thuneberg, and G. S. Paraoanu, *New J. Phys.* **17**, 043058 (2015).
- [8] G. Sun, X. Wen, Y. Wang, S. Cong, J. Chen, L. Kang, W. Xu, Y. Yu, S. Han, and P. Wu, *App. Phys. Lett.* **94**, 102502 (2009).
- [9] M. C. Baruch and T. F. Gallagher, *Phys. Rev. Lett.* **68**, 3515 (1992); S. Yoakum, L. Sirko, and P. M. Koch, *Phys. Rev. Lett.* **69**, 1919 (1992).
- [10] S. Kling, T. Salger, C. Grossert, and M. Weitz, *Phys. Rev. Lett.* **105**, 215301 (2010); A. Zenesini, D. Ciampini, O. Morsch, and E. Arimondo, *Phys. Rev. A* **82**, 065601 (2010).
- [11] A. Das, *Phys. Rev. B* **82**, 172402 (2010); S. Bhattacharyya, A. Das, and S. Dasgupta, *Phys. Rev. B* **86**, 054410 (2012).
- [12] A. Russomanno, A. Silva, and G. E. Santoro, *Phys. Rev. Lett.* **109**, 257201 (2012).
- [13] L. D'Alessio and A. Polkovnikov, *Ann. Phys.* **333**, 19 (2013); M. Bukov, L. D'Alessio, and A. Polkovnikov, *Adv. Phys.* **64**, 139 (2015); T. Nag, S. Roy, A. Dutta, and D. Sen, *Phys. Rev. B* **89**, 165425 (2014).
- [14] P. Ponte, A. Chandran, Z. Papić and D.A. Abanin, *Ann. Phys.* **353** 196 (2015); P. Ponte, Z. Papić, F. Huvneers and D. A. Abanin *Phys. Rev. Lett.* **114**, 140401 (2015); A. Lazarides, A. Das and R. Moessner, *Phys. Rev. Lett.* **115**, 030402 (2015); D. A. Abanin, W. De Roeck, F. Huvneers *Ann. Phys.* **372**, 1 (2016); M. Kozarzewski, P. Prelovšek, M. Mierzejewski, *Phys. Rev. B* **93**, 235151 (2016); J. Rehn, A. Lazarides, F. Pollmann, and R. Moessner, *Phys. Rev. B* **94**, 020201 (2016); S. Gopalakrishnan, M. Knap, and E. Demler, *Phys. Rev. B* **94**, 094201 (2016).
- [15] P. Bordia, H. Lüschen, U. Schneider, M. Knap and I. Bloch, *Nat. Phys.* **13**, 463 (2017).
- [16] A. Lazarides, A. Das, and R. Moessner, *Phys. Rev. Lett.* **112**, 150401 (2014); J. Eisert, M. Friesdorf, and C. Gogolin, *Nat. Phys.* **11**, 124 (2015); R. Moessner and S. L. Sondhi, *Nat. Phys.* **13**, 424 (2017).
- [17] N. Goldman, J. C. Budich, and P. Zoller, *Nat Phys* **12**, 639 (2016); N. Goldman and J. Dalibard, *Phys. Rev. X* **4**, 031027 (2014); M. Bukov, L. D'Alessio, and A. Polkovnikov, *Adv. Phys.* **64**, 139 (2015); A. Eckardt, *Rev. Mod. Phys.* **89**, 011004 (2017). T. Kitagawa, E. Berg, M. Rudner, and E. Demler, *Phys. Rev. B* **82** 235114 (2010); V. Khemani, A. Lazarides, R. Moessner, and S. L. Sondhi, *Phys. Rev. Lett.* **116**, 250401 (2016); D. V. Else and C. Nayak, *Phys. Rev. B* **93**, 201103 (2016); C. W. von Keyserlingk and S. L. Sondhi, *Phys. Rev. B* **93**, 245145 (2016); C. W. von Keyserlingk and S. L. Sondhi, *Phys. Rev. B* **93**, 245146 (2016); A. C. Potter, T. Morimoto and A. Vishwanath, *Phys. Rev. X* **6**, 041001 (2016).
- [18] F. Wilczek, *Phys. Rev. Lett.* **109**, 160401 (2012); D. V. Else, B. Bauer, and C. Nayak *Phys. Rev. Lett.* **117**, 090402 (2016); J. Zhang *et al.*, *Nature* **543**, 217 (2017); N. Y. Yao, A. C. Potter, I.-D. Potirniche, and A. Vishwanath *Phys. Rev. Lett.* **118**, 269901 (2017).
- [19] M. Saffman, T. G. Walker, and K. Mølmer, *Rev. Mod. Phys.* **82**, 2313 (2010); M. P. A. Jones, L. G. Marcassa, and J. P. Shaffer, *J. Phys. B: At., Mol. Opt. Phys.* **50**, 060202 (2017).
- [20] T. Pohl, E. Demler, and M. D. Lukin, *Phys. Rev. Lett.* **104**, 043002 (2010); H. Weimer and H. P. Büchler, *Phys. Rev. Lett.* **105**, 230403 (2010); H. Weimer, R. Löw, T. Pfau, and H. P. Büchler, *Phys. Rev. Lett.* **101**, 250601 (2008); R. Löw, H. Weimer, U. Krohn, R. Heidemann, V. Bendkowsky, B. Butscher, H. P. Büchler, and T. Pfau, *Phys. Rev. A* **80**, 033422 (2009); H. Weimer, M. Müller, I. Lesanovsky, P. Zoller, and H. P. Büchler, *Nat. Phys.* **6**, 382 (2010); B. Olmos, R. González-Férez, and I. Lesanovsky, *Phys. Rev. Lett.* **103**, 185302 (2009); S. Ji, C. Ates, and I. Lesanovsky, *Phys. Rev. Lett.* **107**, 060406; A. W. Glaetzle, K. Ender, D. S. Wild, S. Choi, H. Pichler, M. D. Lukin, and P. Zoller, *Phys. Rev. X* **7**, 031049 (2017). (2011); I. Lesanovsky, *Phys. Rev. Lett.* **106**, 025301 (2011); M. Marcuzzi, J. c. v. Minár D. Barredo, S. de Léséleuc, H. Labuhn, T. Lahaye, A. Browaeys, E. Levi, and I. Lesanovsky, *Phys. Rev. Lett.* **118**, 063606 (2017); A. W. Glaetzle, M. Dalmonte, R. Nath, C. Gross, I. Bloch and P. Zoller, *Phys. Rev. Lett.* **114**, 173002 (2015).
- [21] S. Helmrich, A. Arias, and S. Whitlock, arXiv:1605.08609; A. Piñeiro Orioli, A. Signoles, H. Wildhagen, G. Günter, J. Berges, S. Whitlock, and M. Weidemüller, arXiv:1703.05957; P. Schauß, J. Zeiher, T. Fukuhara, S. Hild, M. Cheneau, T. Macrì, T. Pohl, I. Bloch, and C. Gross, *Science* **347**, 1455 (2015); Y. Y. Jau, A. M. Hankin, T. Keating, I. H. Deutsch, and G. W. Biedermann, *Nat. Phys.* **12**, 71 (2016); N. Takei, C. Sommer, C. Genes, G. Pupillo, H. Goto, K. Koyasu, H. Chiba, M. Weidemüller, and K. Ohmori, *Nat. Comm.* **7**, 13449 (2016); J. Zeiher, R. van Bijnen, P. Schausz, S. Hild, J.-y. Choi, T. Pohl, I. Bloch, and C. Gross, *Nat. Phys.* **12**, 1095 (2016).
- [22] H. Labuhn, D. Barredo, S. Ravets, S. de Léséleuc, T. Macrì, T.

- Lahaye, and A. Browaeys, *Nature* **534**, 667 (2016); D. Barredo, H. Labuhn, S. Ravets, T. Lahaye, A. Browaeys, and C. S. Adams, *Phys. Rev. Lett.* **114**, 113002 (2015).
- [23] J. Zeiher, J.-y. Choi, A. Rubio-Abadal, T. Pohl, R. v. Bijnen, I. Bloch, and C. Gross, arXiv:1705.08372.
- [24] W. R. Anderson, J. R. Veale, and T. F. Gallagher, *Phys. Rev. Lett.* **80**, 249 (1998); I. Mourachko, D. Comparat, F. de Tomasi, A. Fioretti, P. Nosbaum, V. M. Akulin, and P. Pillet, *Phys. Rev. Lett.* **80**, 253 (1998).
- [25] M. D. Lukin, M. Fleischhauer, R. Cote, L. M. Duan, D. Jaksch, J. I. Cirac, and P. Zoller, *Phys. Rev. Lett.* **87**, 037901 (2001).
- [26] E. Urban, T. A. Johnson, T. Henage, L. Isenhower, D. D. Yavuz, T. G. Walker, and M. Saffman, *Nat. Phys.* **5**, 110 (2009); A. Gaetan, Y. Miroshnychenko, T. Wilk, A. Chotia, M. Viteau, D. Comparat, P. Pillet, A. Browaeys, and P. Grangier, *Nat. Phys.* **5**, 115 (2009).
- [27] R. Heidemann, U. Raitzsch, V. Bendkowsky, B. Butscher, R. Löw, L. Santos, and T. Pfau, *Phys. Rev. Lett.* **99**, 163601 (2007).
- [28] C. Ates, T. Pohl, T. Pattard, and J. M. Rost, *Phys. Rev. Lett.* **98**, 023002 (2007); T. Amthor, C. Giese, C. S. Hofmann, and M. Weidemüller, *Phys. Rev. Lett.* **104**, 013001 (2010).
- [29] J. Qian, Y. Qian, M. Ke, X. L. Feng, C. H. Oh, and Y. Z. Wang, *Phys. Rev. A* **80**, 053413 (2009).
- [30] S. Baier, M. J. Mark, D. Petter, K. Aikawa, L. Chomaz, Z. Cai, M. Baranov, P. Zoller and F. Ferlaino, *Science* **352** 201 (2016); M. F. Jürgensen, M. J. Mark, H. C. Nägerl and D. S. Lühmann *Phys. Rev. Lett.* **113** 193003 (2014); T. Sowiński, O. Dutta, P. Hauke, L. Tagliacozzo, and M. Lewenstein, *Phys. Rev. Lett.* **108**, 115301 (2012); O. Dutta, M. Gajda, P. Hauke, M. Lewenstein, D. Lühmann, B. A. Malomed, T. Sowiński and J. Zakrzewski, *Rep. Prog. Phys.* **78**, 066001 (2015).
- [31] M. Bukov, M. Kolodrubetz, and A. Polkovnikov, *Phys. Rev. Lett.* **116**, 125301 (2016);
- [32] L. Béguin, A. Vernier, R. Chicireanu, T. Lahaye, and A. Browaeys, *Phys. Rev. Lett.* **110**, 263201 (2013).
- [33] Refer supplemental material.
- [34] S. Ashhab, J. R. Johansson, A. M. Zagoskin, and F. Nori, *Phys. Rev. A* **75**, 063414 (2007).
- [35] L. D'Alessio and M. Rigol, *Phys. Rev. X* **4**, 041048 (2014)
- [36] The resonances for $N = 3$ are given in the supplemental material.
- [37] H. Lignier, C. Sias, D. Ciampini, Y. Singh, A. Zenesini, O. Morsch, and E. Arimondo, *Phys. Rev. Lett.* **99**, 220403 (2007).
- [38] E. J. Torres-Herrera and L. F. Santos, *Phys. Rev. A* **89**, 043620 (2014).
- [39] M. Calixto and E. Romera, *J. Stat. Mech.* P06029 (2015).
- [40] Similar Gaussian decay is obtained for the fidelity $|\langle I|\psi(t)\rangle|^2$.
- [41] I. I. Beterov, I. I. Ryabtsev, D. B. Tretyakov, and V. M. Entin, *Phys. Rev. A* **79**, 052504 (2009).
- [42] P. Schau, M. Cheneau, M. Endres, T. Fukuhara, S. Hild, A. Omran, T. Pohl, C. Gross, S. Kuhr, I. Bloch, *Nature* **491** 87 (2012).

Supplemental Material for: Periodically Driven Array of Single Rydberg Atoms

Sagarika Basak, Yashwant Chougale and Rejish Nath

Indian Institute of Science Education and Research, Pune 411 008, India

HAMILTONIAN IN THE ROTATING FRAME: SCHRIEFFER-WOLF TRANSFORMATION

Introducing Schrieffer-Wolf Transformation defined by the unitary operator, $\hat{U}(t) = \exp[i f(t) \sum_j \hat{\sigma}_{ee}^j + it \sum_{j < k} V_{jk} \hat{\sigma}_{ee}^j \hat{\sigma}_{ee}^k]$ with $f(t) = \delta/\omega_0 \cos \omega_0 t - \Delta_0 t$, the Hamiltonian

$$\hat{H} = -\Delta(t) \sum_{i=1}^N \hat{\sigma}_{ee}^i + \frac{\Omega}{2} \sum_{i=1}^N (\hat{\sigma}_{eg}^i + \hat{\sigma}_{ge}^i) + \sum_{i < j} V_{ij} \hat{\sigma}_{ee}^i \hat{\sigma}_{ee}^j, \quad (8)$$

$$e^{it/2 \sum_{j,k}^{j \neq k} V_{jk} \hat{\sigma}_{ee}^j \hat{\sigma}_{ee}^k} \left(e^{if(t)} \hat{\sigma}_{eg}^l + e^{-if(t)} \hat{\sigma}_{ge}^l \right) e^{-it/2 \sum_{j,k}^{j \neq k} V_{jk} \hat{\sigma}_{ee}^j \hat{\sigma}_{ee}^k} = e^{it \sum_j^{j \neq l} V_{jl} \hat{\sigma}_{ee}^j \hat{\sigma}_{ee}^l} \left(e^{if(t)} \hat{\sigma}_{eg}^l + e^{-if(t)} \hat{\sigma}_{ge}^l \right) e^{-it \sum_j^{j \neq l} V_{jl} \hat{\sigma}_{ee}^j \hat{\sigma}_{ee}^l}, \quad (11)$$

where the double summation in the exponential function has reduced to a single one in the last step. Then, using Baker-Hausdorff lemma we get,

$$\begin{aligned} & e^{it \sum_j^{j \neq l} V_{jl} \hat{\sigma}_{ee}^j \hat{\sigma}_{ee}^l} \left(e^{if(t)} \hat{\sigma}_{eg}^l + e^{-if(t)} \hat{\sigma}_{ge}^l \right) e^{-it \sum_j^{j \neq l} V_{jl} \hat{\sigma}_{ee}^j \hat{\sigma}_{ee}^l} \\ &= e^{i[f(t)+t \sum_{j \neq l} V_{lj} \hat{\sigma}_{ee}^j]} \hat{\sigma}_{eg}^l + e^{-i[f(t)+t \sum_{j \neq l} V_{lj} \hat{\sigma}_{ee}^j]} \hat{\sigma}_{ge}^l, \quad (12) \end{aligned}$$

which then finally gives us,

$$\hat{H}' = \frac{\Omega}{2} \sum_{j=1}^N \sum_{m=-\infty}^{\infty} i^m J_m(\alpha) e^{i(m\omega_0 - \Delta_0 + \sum_{k \neq j} V_{jk} \hat{\sigma}_{ee}^k)t} \hat{\sigma}_{eg}^j + \text{H.c.} \quad (13)$$

where $J_m(\alpha)$ is the m th order Bessel function with $\alpha = \delta/\omega_0$. Using $e^{\pm i \sum_{k \neq j} V_{jk} \hat{\sigma}_{ee}^k t} = \prod_{k \neq j} [\hat{\sigma}_{ee}^k (e^{\pm i t V_{jk}} - 1) + \mathcal{I}]$, where \mathcal{I} is

transforms as $\hat{H}'(t) = \hat{U}(t) \hat{H}(t) \hat{U}^\dagger(t) - i\hbar \hat{U}(t) \dot{\hat{U}}^\dagger(t)$. The final Hamiltonian is

$$\hat{H}'(t) = \frac{\Omega}{2} \hat{U}(t) \sum_{i=1}^N (\hat{\sigma}_{eg}^i + \hat{\sigma}_{ge}^i) \hat{U}^\dagger(t). \quad (9)$$

To evaluate $\hat{H}'(t)$, we need the following terms:

$$e^{if(t) \hat{\sigma}_{ee}^i} (\sigma_{eg}^i + \sigma_{ge}^i) e^{-if(t) \hat{\sigma}_{ee}^i} = e^{if(t)} \sigma_{eg}^i + e^{-if(t)} \sigma_{ge}^i \quad (10)$$

and

the identity operator, we can rewrite the Hamiltonian as

$$\begin{aligned} \hat{H}'(t) &= \frac{\Omega}{2} \sum_j^N \sum_{m=-\infty}^{\infty} i^m J_m(\alpha) \left[g(t) \hat{\sigma}_{eg}^j \left(\prod_{k \neq j} [\hat{\sigma}_{ee}^k (e^{it V_{jk}} - 1) + \mathcal{I}] \right) \right. \\ &\quad \left. + g^*(t) \hat{\sigma}_{ge}^j \left(\prod_{k \neq j} [\hat{\sigma}_{ee}^k (e^{-it V_{jk}} - 1) + \mathcal{I}] \right) \right], \quad (14) \end{aligned}$$

where $g(t) = \exp[i(m\omega_0 - \Delta_0)t]$. The Eq. (14) for $N = 2$ is discussed in the main text in detail.

NEAREST NEIGHBOUR APPROXIMATION: TIME INDEPENDENT HAMILTONIAN

We truncate the interactions beyond nearest neighbour, and then calculate the time independent average Hamiltonian, $H_{eff} = 1/T \int_0^T dt \hat{H}'(t)$ where $T = 2\pi/\omega_0$ if $\omega_0 \gg V_0$ or $T = 2\pi/V_0$ if $V_0 \gg \omega_0$. Up to nearest neighbour interactions, Eq. (14) reduces to

$$\begin{aligned} \hat{H}'_{NN}(t) &= \frac{\Omega}{2} \sum_j^N \sum_{m=-\infty}^{\infty} i^m J_m(\alpha) g(t) \hat{\sigma}_{eg}^j \left[1 + \hat{\sigma}_{ee}^{j+1} \hat{\sigma}_{ee}^{j-1} (e^{iV_0 t} - 1) \right. \\ &\quad \left. + (\hat{\sigma}_{ee}^{j+1} + \hat{\sigma}_{ee}^{j-1}) (e^{iV_0 t} - 1) \right] + \text{H.c.} \quad (15) \end{aligned}$$

Case 1: The effective time independent Hamiltonian up to the nearest neighbour interaction V_0 for $\omega_0 \gg V_0$:

$$\begin{aligned} \hat{H}_{eff}^{\omega_0 \gg V_0} = & \frac{\Omega}{2iT} \sum_j \sum_{m=-\infty}^{\infty} i^m J_m(\alpha) \left[\frac{(e^{-i\Delta_0 T} - 1)}{m\omega_0 - \Delta_0} (1 - \hat{\sigma}_{ee}^{j+1} - \hat{\sigma}_{ee}^{j-1} + \hat{\sigma}_{ee}^{j+1} \hat{\sigma}_{ee}^{j-1}) + \frac{(e^{-i(\Delta_0 - 2V_0)T} - 1)}{m\omega_0 - \Delta_0 + 2V_0} \hat{\sigma}_{ee}^{j+1} \hat{\sigma}_{ee}^{j-1} \right. \\ & \left. + \frac{(e^{-i(\Delta_0 - V_0)T} - 1)}{m\omega_0 - \Delta_0 + V_0} (\hat{\sigma}_{ee}^{j+1} + \hat{\sigma}_{ee}^{j-1} - 2\hat{\sigma}_{ee}^{j+1} \hat{\sigma}_{ee}^{j-1}) \right] \hat{\sigma}_{eg}^j + \text{H.c.} \end{aligned} \quad (16)$$

For $\Delta_0 = 0$, it becomes

$$\begin{aligned} \hat{H}_{eff}^{\omega_0 \gg V_0} = & \frac{\Omega}{2iT} \sum_j \sum_{m=-\infty}^{\infty} i^m J_m(\alpha) \left[\frac{(e^{i2V_0 T} - 1)}{m\omega_0 + 2V_0} \hat{\sigma}_{ee}^{j+1} \hat{\sigma}_{ee}^{j-1} + \frac{(e^{iV_0 T} - 1)}{m\omega_0 + V_0} (\hat{\sigma}_{ee}^{j+1} + \hat{\sigma}_{ee}^{j-1} - 2\hat{\sigma}_{ee}^{j+1} \hat{\sigma}_{ee}^{j-1}) \right] \hat{\sigma}_{eg}^j \\ & + \frac{J_0(\alpha)\Omega}{2} \sum_{j=1}^N \hat{\sigma}_{eg}^j (1 - \hat{\sigma}_{ee}^{j+1} - \hat{\sigma}_{ee}^{j-1} + \hat{\sigma}_{ee}^{j+1} \hat{\sigma}_{ee}^{j-1}) + \text{H.c.}, \end{aligned} \quad (17)$$

Now, for $V_0 \ll \Omega$, the Eq. (17) becomes

$$\begin{aligned} \hat{H}_{eff}^{\omega_0 \gg V_0} = & \frac{\Omega}{2} \sum_j \sum_{m=-\infty}^{\infty} i^m J_m(\alpha) \left[\frac{-2V_0^2}{(m\omega_0 + 2V_0)(m\omega_0 + V_0)} \hat{\sigma}_{ee}^{j+1} \hat{\sigma}_{ee}^{j-1} + \frac{V_0}{m\omega_0 + V_0} (\hat{\sigma}_{ee}^{j+1} + \hat{\sigma}_{ee}^{j-1}) \right] \hat{\sigma}_{eg}^j \\ & + \frac{J_0(\alpha)\Omega}{2} \sum_{j=1}^N \hat{\sigma}_{eg}^j (1 - \hat{\sigma}_{ee}^{j+1} - \hat{\sigma}_{ee}^{j-1} + \hat{\sigma}_{ee}^{j+1} \hat{\sigma}_{ee}^{j-1}) + \text{H.c.}, \end{aligned} \quad (18)$$

Writing Eq. (18) for $N = 2$:

$$\begin{aligned} \hat{H}_{eff}^{\omega_0 \gg V_0} = & \frac{\Omega}{2} \sum_{m=-\infty}^{\infty} i^m J_m(\alpha) \left[\frac{V_0}{m\omega_0 + V_0} (\hat{\sigma}_{eg}^1 \hat{\sigma}_{ee}^2 + \hat{\sigma}_{eg}^2 \hat{\sigma}_{ee}^1) \right] \\ & + \frac{J_0(\alpha)\Omega}{2} \left(\sum_{j=1}^2 \hat{\sigma}_{eg}^j - \hat{\sigma}_{eg}^1 \hat{\sigma}_{ee}^2 - \hat{\sigma}_{eg}^2 \hat{\sigma}_{ee}^1 \right) + \text{H.c.} \end{aligned} \quad (19)$$

Case 2: Similarly, for $V_0 \gg \omega_0$:

$$\hat{H}_{eff}^{V_0 \gg \omega_0} = \frac{\Omega}{2iT} \sum_j \sum_{m=-\infty}^{\infty} i^m J_m(\alpha) (g(T) - 1) \left[\frac{(1 - \hat{\sigma}_{ee}^{j+1} - \hat{\sigma}_{ee}^{j-1} + \hat{\sigma}_{ee}^{j+1} \hat{\sigma}_{ee}^{j-1})}{m\omega_0 - \Delta_0} + \frac{\hat{\sigma}_{ee}^{j+1} \hat{\sigma}_{ee}^{j-1}}{m\omega_0 - \Delta_0 + 2V_0} + \frac{(\hat{\sigma}_{ee}^{j+1} + \hat{\sigma}_{ee}^{j-1} - 2\hat{\sigma}_{ee}^{j+1} \hat{\sigma}_{ee}^{j-1})}{m\omega_0 - \Delta_0 + V_0} \right] \hat{\sigma}_{eg}^j + \text{H.c.} \quad (20)$$

For $\Delta_0 = 0$, Eq. (21) becomes

$$\hat{H}_{eff}^{V_0 \gg \omega_0} = \frac{\Omega}{2iT} \sum_j \sum_{m=-\infty}^{\infty} i^m J_m(\alpha) (e^{im\omega_0 T} - 1) \left[\frac{(1 - \hat{\sigma}_{ee}^{j+1} - \hat{\sigma}_{ee}^{j-1} + \hat{\sigma}_{ee}^{j+1} \hat{\sigma}_{ee}^{j-1})}{m\omega_0} + \frac{\hat{\sigma}_{ee}^{j+1} \hat{\sigma}_{ee}^{j-1}}{m\omega_0 + 2V_0} + \frac{(\hat{\sigma}_{ee}^{j+1} + \hat{\sigma}_{ee}^{j-1} - 2\hat{\sigma}_{ee}^{j+1} \hat{\sigma}_{ee}^{j-1})}{m\omega_0 + V_0} \right] \hat{\sigma}_{eg}^j + \text{H.c.} \quad (21)$$

For $N = 2$, we have

$$\hat{H}_{eff}^{V_0 \gg \omega_0} = \frac{\Omega}{2iT} \sum_{m=-\infty}^{\infty} i^m J_m(\alpha) (e^{im\omega_0 T} - 1) \left[\sum_{j=1}^2 \frac{\hat{\sigma}_{eg}^j}{m\omega_0} + \left(\frac{1}{m\omega_0 + V_0} - \frac{1}{m\omega_0} \right) \hat{X} \right] + \text{H.c.} \quad (22)$$

TRANSVERSE MATRIX APPROACH FOR TWO INTERACTING RYDBERG ATOMS

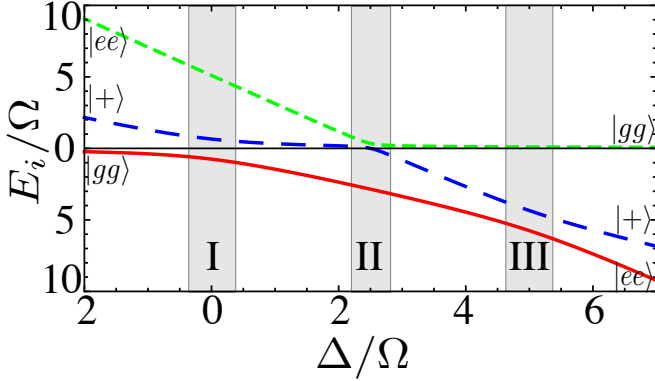


Figure 6. (color online). The energy levels vs Δ obtained by diagonalizing the Hamiltonian in Eq. 1 with $\delta = 0$ and $V_0/\hbar\Omega = 5$, in the basis $\{|gg\rangle, |+\rangle, |ee\rangle\}$. The asymptotic states are also shown in the figure. The three shaded regions are the different LZT regions asymptotically corresponds to (I) $|gg\rangle \leftrightarrow |+\rangle$, (II) $|gg\rangle \leftrightarrow |ee\rangle$ and (III) $|+\rangle \leftrightarrow |ee\rangle$.

The energy level diagram as a function of Δ in the non-driven case ($\delta = 0$) is shown in Fig. 5 for $V_0 = 5\Omega$. We consider each of the LZT points separately.

First transition: $|gg\rangle \leftrightarrow |+\rangle$

Under strong driving, the LZT matrix written in the basis $\{|gg\rangle, |+\rangle, |ee\rangle\}$ is,

$$G_{LZ,k}^{gg \rightarrow +} = \begin{bmatrix} \cos \chi_1/2 & -e^{i\theta_{LZ,k}} \sin \chi_1/2 & 0 \\ e^{-i\theta_{LZ,k}} \sin \chi_1/2 & \cos \chi_1/2 & 0 \\ 0 & 0 & 0 \end{bmatrix}$$

where k is the direction of the sweep across the crossing: for $k = 1$, $\Delta(t)$ goes from +ve to -ve and viceversa for $k = 2$. The sweep rates are direction independent. Hence, χ_1 is independent of k and $\cos^2 \chi_1/2 = e^{-\pi\Omega^2/v_1}$, where $v_1 = \omega_0 \sqrt{\delta^2 - \Delta_0^2}$ is the rate at which the atom is swept through the avoided level crossing and is obtained by linearizing the \hat{H} around the LZT point. The boundary independent phases acquired during the LZT are: $\theta_{LZ,1} = \pi - \phi_S$ and $\theta_{LZ,2} = \phi_S$, where the Stokes phase,

$$\phi_S = \frac{\pi}{4} + \delta' (\ln \delta' - 1) + \arg[\Gamma(1 - i\delta')], \quad (23)$$

with Γ is the gamma function and $\delta' = \Omega^2/2v$. ϕ_S approaches $\frac{\pi}{4}$ in the diabatic limit and 0 in the adiabatic limit. Away from the LZT region, the states acquire a relative phase given by the adiabatic matrix

$$G_j^{gg \rightarrow +} = \begin{bmatrix} e^{-i\theta_j} & 0 & 0 \\ 0 & e^{i\theta_j} & 0 \\ 0 & 0 & 1 \end{bmatrix}.$$

If $\Delta_0 \neq 0$, there are two phase factors corresponding to the system being on the right or left side of the crossing region. Finally, the evolution matrix for one full cycle is $G = G_{LZ,2}^{gg \rightarrow +} G_2 G_{LZ,1}^{gg \rightarrow +} G_1$. Rewriting as, $\hat{G} = \hat{G}_{xy} \hat{G}_z$ where \hat{G}_{xy} and \hat{G}_z are respectively represent rotations about an axis lying in the xy plane and z axis [34]. The former introduces the population transfer between the diabatic states, and the latter is just an overall phase matrix with diagonal elements. In FPL, the overall phase matrix can be approximated as $\{e^{-i(\theta_1+\theta_2)}, e^{i(\theta_1+\theta_2)}, 1\}$. The complete population transfer between the states happens, i.e. the resonance occurs when $\theta_1 + \theta_2 = 2n\pi$ (constructive interference), which then gives us the S resonance condition: $\Delta_0 = n\omega_0$.

Second transition: $|gg\rangle \leftrightarrow |ee\rangle$

The population transfer from $|gg\rangle$ to $|ee\rangle$ takes place through the $|+\rangle$ state. Hence, the landau zener matrix is the product of the two landau zener matrices defined for ground to plus and plus to excited state:

$$G_{LZ,k}^{gg \rightarrow ee} = G_{LZ,k}^{+ \rightarrow ee} \cdot G_{LZ,k}^{gg \rightarrow +}$$

Here, the adiabatic phase matrix is given by,

$$G_j^{gg \rightarrow ee} = \begin{bmatrix} e^{-i\theta_j} & 0 & 0 \\ 0 & e^{-i(\kappa_j+\theta_j)} & 0 \\ 0 & 0 & e^{i\kappa_j} \end{bmatrix}$$

where κ_j is the adiabatic phase acquired away from the $|+\rangle$ to $|ee\rangle$ avoided crossing. Finally, after doing similar analysis like the first transition we arrive at the resonance condition: $\Delta_0 - V_0/2 = n\omega_0$.

Third transition: $|+\rangle \leftrightarrow |ee\rangle$

The LZT matrix attained for this transition is,

$$G_{LZ,k}^{+ \rightarrow ee} = \begin{bmatrix} 0 & 0 & 0 \\ 0 & \cos \chi_2/2 & -e^{i\theta_{LZ,k}} \sin \chi_2/2 \\ 0 & e^{-i\theta_{LZ,k}} \sin \chi_2/2 & \cos \chi_2/2 \end{bmatrix}$$

where $\cos^2 \chi_2/2 = e^{-\pi\Omega^2/v_2}$ with the sweep rate at the LZ crossing, $v_2 = \omega_0 \sqrt{\delta^2 - (\Delta_0 - V)^2}$. The phase matrix attained is,

$$G_j^{+ \rightarrow ee} = \begin{bmatrix} 1 & 0 & 0 \\ 0 & e^{-i\kappa_j} & 0 \\ 0 & 0 & e^{i\kappa_j} \end{bmatrix}$$

A similar analysis as above, gives us a resonance condition: $\Delta_0 - V_0 = n\omega_0$.

DIFFERENT RESONANCES FOR $N = 3$

There are a total of 9 resonances in a 3-atom lattice. They are:

Transition	Resonance condition
$ ggg\rangle \leftrightarrow gge\rangle, geg\rangle, egg\rangle$	$n\omega_0 = \Delta_0$
$ ggg\rangle \leftrightarrow gee\rangle, eeg\rangle$	$n\omega_0 = \Delta_0 - V_0/2$
$ ggg\rangle \leftrightarrow ege\rangle$	$n\omega_0 = \Delta_0 - V_0/128$
$ ggg\rangle \leftrightarrow eee\rangle$	$n\omega_0 = \Delta_0 - 2V_0/3 - V_0/192$
$ gge\rangle, geg\rangle, egg\rangle \leftrightarrow gee\rangle, eeg\rangle$	$n\omega_0 = \Delta_0 - V_0$
$ gge\rangle, geg\rangle, egg\rangle \leftrightarrow ege\rangle$	$n\omega_0 = \Delta_0 - V_0/64$
$ gge\rangle, geg\rangle, egg\rangle \leftrightarrow eee\rangle$	$n\omega_0 = \Delta_0 - V_0 - V_0/128$
$ gee\rangle, eeg\rangle \leftrightarrow eee\rangle$	$n\omega_0 = \Delta_0 - V_0 - V_0/64$
$ ege\rangle \leftrightarrow eee\rangle$	$n\omega_0 = \Delta_0 - 2V_0$

If the interactions are small, all of them overlap with each other.

Dissipative dynamics

To study the effect of spontaneous emission on the two atoms correlated dynamics, we introduce the master equations for the two-particle density matrix,

$$\partial_t \hat{\rho} = -i [\hat{H}, \hat{\rho}] + \mathcal{L}[\hat{\rho}], \quad (24)$$

with the Lindblad operator given by

$$\mathcal{L}[\hat{\rho}] = \sum_{i=1}^2 \hat{C}_i \hat{\rho} \hat{C}_i^\dagger - \frac{1}{2} \sum_m (\hat{C}_i^\dagger \hat{C}_i \hat{\rho} + \hat{\rho} \hat{C}_i^\dagger \hat{C}_i) \quad (25)$$

where the operator, $\hat{C}_i = \sqrt{\Gamma} \hat{\sigma}_{ge}^i$ with Γ is the spontaneous decay rate of the excited state $|e\rangle$. The results for blockade enhancement and anti-blockade at large interactions are shown in Fig. 7 for $N = 2$.

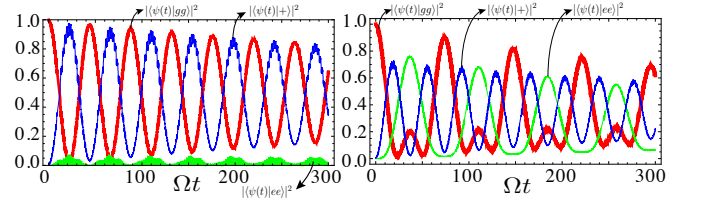


Figure 7. (color online). (a) The blockade enhancement at $V_0 = 0.5\Omega$ and (b) anti-blockade dynamics at $V_0 = 6\Omega$ for $N = 2$, $\omega_0 = 3\Omega$, $\delta = 34\Omega$, $\Delta_0 = 0$ and $\Omega = 1\text{MHz}$. The Rydberg state is taken to be $43S_{1/2}$ state, which has a life time of $\sim 100\mu\text{s}$.